The human GFI136N variant induces epigenetic changes at the *Hoxa9* locus and accelerates K-RAS driven myeloproliferative disorder in mice

Cyrus Khandanpour,[1,2] *Joseph Krongold,[1] *Judith Schütte,[3] Frederique Bouwman,[1] Lothar Vassen,[1] Marie-Claude Gaudreau,[1,4] Riyan Chen,[1] Fernando J. Calero-Nieto,[3] Evangelia Diamanti,[3] Rebecca Hannah,[3] Sara E. Meyer,[5] H. Leighton Grimes,[5,6] Bert A. van der Reijden,[7] Joop H. Jansen,[7] Chandrashekhar V. Patel,[8] Justine K. Peeters,[9] Bob Löwenberg,[9] Ulrich Dührsen,[2] Bertie Göttgens,[3] and Tarik Möröy[1,4]

[1]Institut de recherches cliniques de Montréal, Montreal, QC; [2]Westdeutsches Tumorzentrum Klinik für Hämatologie Universitätsklinikum Essen, Essen, Germany; [3]Cambridge University, Department of Haematology, Cambridge Institute for Medical Research, Cambridge, United Kingdom; [4]Département de Microbiologie et Immunologie, Université de Montreal, Montreal, QC; [5]Division of Immunobiology, Cincinnati Children's Hospital Medical Center, Cincinnati, OH; [6]Division of Experimental Hematology, Cincinnati Children's Hospital Medical Center, Cincinnati, OH; [7]Laboratory of Hematology, Department of Laboratory Medicine, Nijmegen Centre for Molecular Life Sciences, Radboud University Nijmegen Medical Centre, Nijmegen, The Netherlands; [8]Department of Cell Biology & Anatomy, University of South Carolina School of Medicine, Columbia, SC; and [9]Department of Hematology, Erasmus University Medical Center, Rotterdam, The Netherlands

The coding single nucleotide polymorphism GFI136N in the human gene growth factor independence 1 (GFI1) is present in 3%-7% of whites and increases the risk for acute myeloid leukemia (AML) by 60%. We show here that GFI136N, in contrast to GFI136S, lacks the ability to bind to the Gfi1 target gene that encodes the leukemia-associated transcription factor *Hoxa9* and fails to initiate histone modifications that regulate *HoxA9* expression. Consistent with this, AML patients heterozygous for the *GFI136N* variant show increased *HOXA9* expression compared with normal controls. Using ChipSeq, we demonstrate that GFI136N specific epigenetic changes are also present in other genes involved in the development of AML. Moreover, granulomonocytic progenitors, a bone marrow subset from which AML can arise in humans and mice, show a proliferative expansion in the presence of the GFI136N variant. In addition, granulomonocytic progenitors carrying the GFI136N variant allele have altered gene expression patterns and differ in their ability to grow after transplantation. Finally, GFI136N can accelerate a K-RAS driven fatal myeloproliferative disease in mice. Our data suggest that the presence of a GFI136N variant allele induces a preleukemic state in myeloid precursors by deregulating the expression of Hoxa9 and other AML-related genes. (*Blood*. 2012;120(19):4006-4017)

Introduction

Gfi1 is a DNA binding transcriptional repressor that recognizes specific target genes via its C-terminal C_2H_2 zinc finger domains. Gfi1 plays an important role in hematopoietic stem cell (HSC) function and B- and T-cell differentiation.[1,2] It is also an important factor for myeloid differentiation because *Gfi1*$^{-/-}$ mice have increased numbers of myeloid precursors, such as granulomonocytic progenitors (GMPs) and common myeloid progenitors (CMPs), accumulate aberrant monocytes and lack neutrophil granulocytes,[3-7] and in humans loss of function mutations in GFI1 cause severe congenital neutropenia.[8] A number of studies suggest that acute myeloid leukemia (AML) cells originate both in human and mice from the CMP, GMP, or lymphoid primed multipotential progenitors (LMPP) fractions.[9-13] Recently, we reported that a single nucleotide polymorphism (SNP) in the GFI1 gene, which leads to the exchange of a serine to an asparagine at position 36, is associated with AML.[14] The *GFI136N* variant allele is present in 3% to 7% of healthy whites and in 11% of AML patients. Persons carrying this SNP have a 1.6-fold increased risk to develop AML compared with persons not carrying this variant. It remains unclear, however, how the AML-associated GFI136N variant can be responsible for this predisposition. To better understand the effects of GFI136N, we have made knock-in mice carrying the human *GFI136N* variant or the more common *GFI136S* form at the endogenous murine *Gfi1* gene locus. This enabled a more detailed investigation of the pathways that are normally regulated by GFI1 in cells expressing the GFI1 variant. Here we present the results that we obtained studying these engineered mice and offer a first mechanistic insight into the function of the GFI136N variant.

Methods

Generation of KI mice

Gfi1$^{36Neo/+}$ or Gfi1$^{36Sneo/+}$ mice were generated following a previously described strategy.[15] All mice were backcrossed to C57Bl/6 background (verified by PCR). All mice were housed under SPF conditions, and the institutional animal ethics committee approved all animal experiments. The following primers were used for genotyping mice: mGfi11, 5′-ccttctctcagaactcagag-3′; mGfi24, 5′-ctggcaagctcagcaaatctg-3′; and R9, 5′-GTTCACA GAAGAGGCCCAGG-3′. The expected knock-in band is at 520 bp, and

Submitted February 10, 2011; accepted August 9, 2012. Prepublished online as *Blood* First Edition paper, August 28, 2012; DOI 10.1182/blood-2011-02-334722.

*J.K. and J.S. contributed equally to this study as second authors.

The online version of this article contains a data supplement.

The publication costs of this article were defrayed in part by page charge payment. Therefore, and solely to indicate this fact, this article is hereby marked "advertisement" in accordance with 18 USC section 1734.

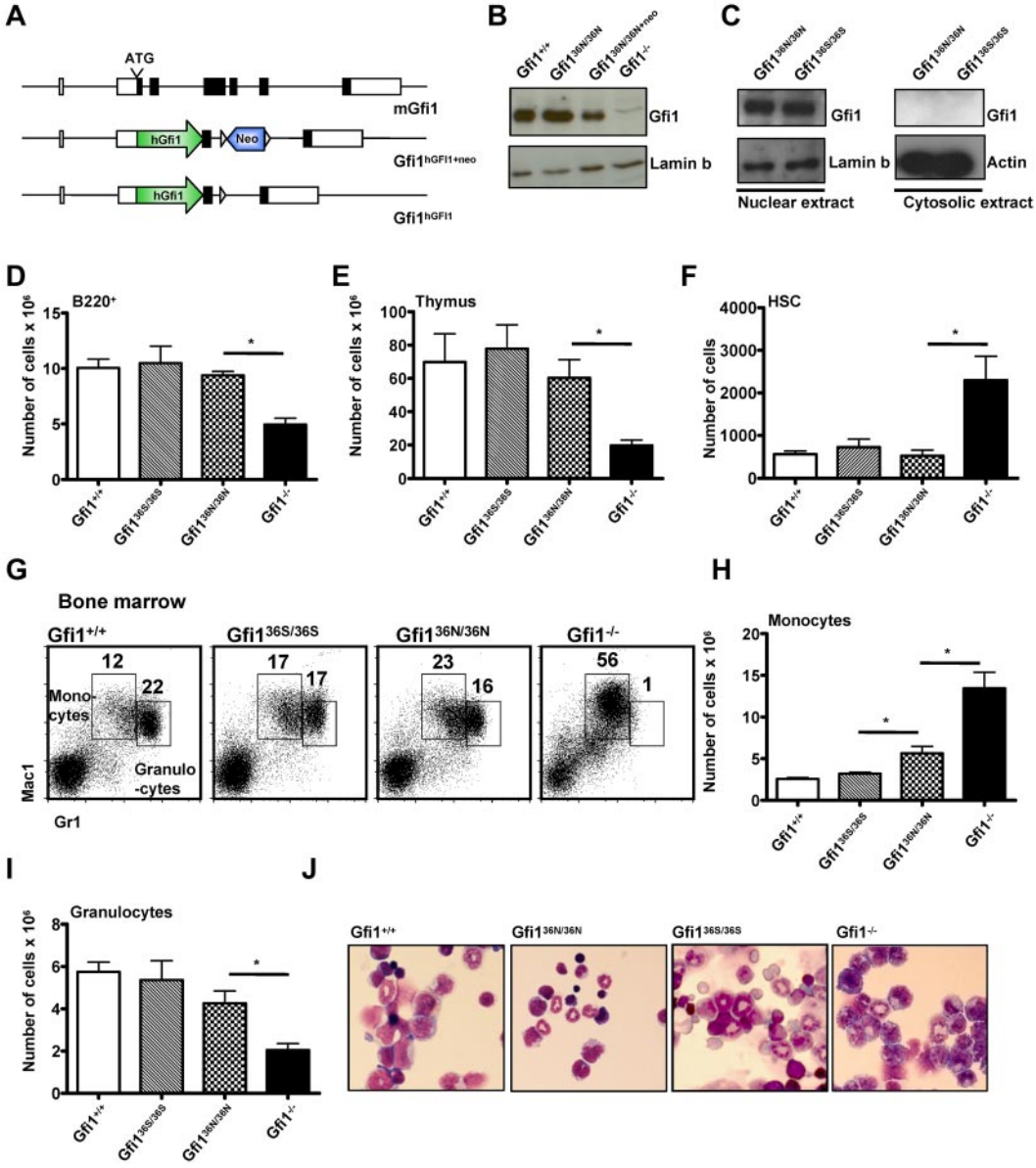

Figure 1. Human GFI1 is equivalent to murine Gfi1 in hematopoiesis. (A) Schematic representation of the murine *Gfi1* locus and the targeted alleles. (B) Western blot of nuclear extracts of *Gfi1*$^{36N/36N}$, *Gfi1*$^{+/+}$, *Gfi1*$^{-/-}$, and *Gfi1*$^{36N/36N+neo}$ thymocytes. (C) Western blot of nuclear and cytosolic extracts of Gfi1$^{36N/36N}$ and Gfi1$^{36S/36S}$ thymocytes. (D) Total number of B220^{+} cells in the bone marrow (per both hind limbs; n = 23 *Gfi1*$^{+/+}$, n = 13 *Gfi1*$^{-/-}$, n = 13 *Gfi1*$^{36N/36N}$, and n = 9 *Gfi1*$^{36S/36S}$). *$P \leq .05$. (E) Total number of thymocytes (n = 9 *Gfi1*$^{+/+}$, n = 5 *Gfi1*$^{-/-}$, n = 5 *Gfi1*$^{36N/36N}$, and n = 6 *Gfi1*$^{36S/36S}$). *$P \leq .05$. (F) Total number of HSCs (Lin^{-}, Kit^{+}, Sca-1^{+}, CD150^{+}, CD48^{-} bone marrow cells) in both hind limbs (n = 15 *Gfi1*$^{+/+}$, n = 7 *Gfi1*$^{-/-}$, n = 3 *Gfi1*$^{36N/36N}$, and n = 4 *Gfi1*$^{36S/36S}$). *$P \leq .05$. (G) Flow cytometric analysis showing the staining of bone marrow cells for Gr1 and Mac1 surface markers. (H) Total number of monocytes in the bone marrow (per both hindlimb; n = 19 *Gfi1*$^{+/+}$, n = 6 *Gfi1*$^{-/-}$, n = 6 *Gfi1*$^{36N/36N}$, and n = 4 *Gfi1*$^{36S/36S}$). *$P \leq .05$. (I) Total number of granulocytes in the bone marrow of the indicated mouse strains per hindlimb (n = 19 Gfi1$^{+/+}$, n = 6 Gfi1$^{-/-}$, n = 6 Gfi1$^{36N/36N}$, and n = 4 *Gfi1*$^{36S/36S}$). *$P \leq .05$. (J) Wright-Giemsa staining of bone marrow cytospins (original magnification ×100, Leitz DMRB from Leica, Micropublisher digital color camera, QImaging, Northern Eclipse Version 7.0 software).

the control wild-type band at 350 bp. Mice were backcrossed to B57L/6J background, and this was verified by background specific satellite PCR.

K-RAS activation and bone marrow transplantation

Expression of a mutated form of K-RAS was induced by injecting the various MxCre tg *K-RAS*^{flstoplfK12D} mice with 500 mg polyriboinosinic acid/polyribocytidylic acid (poly(I:C); Sigma-Aldrich) 3 times every other day.

In vitro colony assay

Approximately 450-500 GMPs were seeded on methylcelluose (Stem Cells, M3434) and expanded further. At day 10, 17, and 24, colonies were counted and replated, and pictures were taken using the Axiovert s100TV microscope.

ChIP

For ChIP with Lin^{-}, Sca1^{-}, ckit^{+} 5×10^5 cells were used, otherwise 5-50 $\times$ 10^6 cells were used. Cells were washed, cross-linked with formaldehyde, and lysed. The collected lysate was sonicated to an average size of 600 bp. Samples were immunoprecipitated with anti-Gfi1 antibody (σ-2.5D) or control antibody and collected with protein G/salmon sperm DNA. Beads were washed and samples were eluted. After reverse-crosslinking, DNA was purified with the Qiaquick PCR Purification Kit (QIAGEN); ~ 5 μL of diluted DNA was used for each real-time PCR reaction. An

Table 1. Myeloid maturation in bone marrow

		Neutrophil maturation, % of all counted cells					
	Myeloblast	Promyelocyte	Myelocyte	Metamyelocyte	Segmented	Monocyte	Lymphocyte
Wt	4 ± 1	2 ± 0.3	12 ± 1	12 ± 2	31 ± 4	6 ± 1	21 ± 5
Gfi1$^{-/-}$	4 ± 1	0.2 ± 0.2	4 ± 1*	2 ± 1*	2 ± 2*	54 ± 12*	10 ± 2*
Gfi1$^{36N/36N}$	2 ± 2	3 ± 1	6 ± 2	10 ± 2	25 ± 3	19 ± 3	31 ± 3
Gfi1$^{36S/36S}$	2 ± 1	1 ± 1	14 ± 7	10 ± 1	16 ± 5	14 ± 3	37 ± 3

Quantification of the different cell types according to their morphology enumerated from bone marrow cytospins of the indicated mouse strains (n = 3 for all genotypes).
*Significant difference to *wt* mouse strain.

α-Gfi1 antibody (2.5D; Sigma-Aldrich) was used for examining binding of Gfi1 to the target genes, as control an α-GFP antibody (sc9996; Santa Cruz Biotechnology) was used. For the H3K4 dimethyl ChIP, a kit (GAM-3203) from SAB-Bioscience was used. For the examination of the Hoxa9 locus, the following primer pairs from SAB Bioscience were used: GPM1052016(+)02A, +1A, −1A, −2A, −3A, and −13A. The primers for the ID2 and Gfi1 have been previously described.[16,17]

Chip seq

ChIP-Seq ChIP assays were performed as previously described[18] using polyclonal anti–dimethyl-histone H3 (Lys4; Millipore 07-030) and anti-Gfi1 (Abcam ab21061) antibodies. Briefly, 5×10^5 $Lin^-Sca1^-cKit^+$ cells and 2×10^7 MLL-ENL–immortalized bone marrow progenitor cells were cross-linked in 1% formaldehyde, lysed and sonicated to fragments of ~ 150-400 bp. Each sample was amplified using the Illumina kit following the manufacturer's instructions and sequenced using the Illumina 2G Genome Analyzer. Sequencing reads were mapped to the mouse reference genome using Bowtie[19] converted to a density plot as described[20] and displayed in the UCSC genome browser. In a first step, reads were normalized as reads per indicated region divided through number of total reads of the genome. In order to take account in different efficiencies of the ChIP, the curves were normalized to genes, which are not Gi1 target genes such as hypoxanthin-phosphoribosyl-transferase (HPRT) or beta-actin. After normalization, the different curves were superimposed and the area under each curve was determined using the TL 100 software from Non-Linear Dynamics. Sequence data have been submitted to the NCBI archive under accession no. GSE31657.

Gene expression array and real-time PCR

Gene expression array was performed according to published procedures.[21] Array data are accessible under GEO Omnibus accession no. 25551. Real-time PCR for Hoxa9 expression in human and murine samples was performed with specific predesigned primers from ABI (human HOXA9 HS00365956_m1 and murine Hoxa9 Mm00439364-m1) according to the manufacturer's instructions.

Statistical analysis

The log-rank test was used for comparing survival rates of mice and the unpaired Student *t* test for analyzing the differences in the number of the different populations. All *P* values were calculated 2-sided. Statistical analysis was done with Prism Version 4 software (GraphPad).

Flow cytometry analysis and sorting of populations

Cells were analyzed and sorted as previously described.[22-24] Lineage-negative cells were defined as the 1% of the live-gated BM cells with the lowest fluorescence of the lineage antibodies.

Reporter assay, methylcellulose assay, and immunoprecipitation

Reporter, methylcellulose, and immunoprecipitation assays were performed as previously described.[14,24]

Patient cohorts

The characteristics of the cohort of patient cohorts from Nijmegen and Rotterdam were previously described.[14] All patient samples were obtained after informed consent according to the Declaration of Helsinki. The respective local ethic committees have approved the use of all patient samples.

Results

Generation of mice carrying the human GFI136N and GFI136S cDNA in the murine Gfi1 locus

To understand how the GFI136N variant contributes to AML development, we used gene targeting to knock-in either the more common GFI136S form (*Gfi1*$^{36S/36S}$) or the GFI136N variant (*Gfi1*$^{36N/36N}$) into the murine *Gfi1* locus (Figure 1A; supplemental Figure 1A-C, available on the *Blood* Web site; see the Supplemental Materials link at the top of the online article). The 2 knock-in strains expressed GFI1 at levels similar to the endogenous murine Gfi1 (Figure 1B-C) and showed no significant difference to *wt* mice with regard to lymphoid differentiation in bone marrow, spleen, and thymus or the number of HSCs (Figure 1D-F; and data not shown). In addition, the cellular composition of the bone marrow and peripheral blood and the number of colony forming cells were also similar to *wt* mice, indicating a functionally intact hematopoiesis in both types of knock-in mice (Tables 1 and 2; supplemental Figure 2).

However, we observed a higher number of monocytes and a tendency toward lower numbers of granulocytes in the *Gfi1*$^{36N/36N}$ mice compared with *Gfi1*$^{36S/36S}$ or *w*t mice, but no obvious difference in cell morphology (Figure 1G-J; Tables 1 and 2). Moreover, significantly increased numbers of GMPs were evident in *Gfi1*$^{36N/36N}$ mice compared with *Gfi1*$^{36S/36S}$ mice or *wt* mice (Figure 2A-B), a phenotype that was similar to the expansion of GMPs previously described in *Gfi1*$^{-/-}$ mice,[4,25] where a higher proportion of GMPs are in $S/G_2/M$ phase compared with *wt* controls because Gfi1 restricts cell cycle progression of these

Table 2. Cellular composition of blood of different mouse strains

	Lymphocytes, %	Neutrophils, %	Monocytes, %	Eosinophils, %	Basophils, %
Wt	62 ± 10	26 ± 7	11 ± 4	1 ± 1	0
Gfi1$^{-/-}$	60 ± 17	1 ± 1*	36 ± 14	2 ± 3	0
Gfi1$^{36N/36N}$	78 ± 5	10 ± 1	9 ± 3	2 ± 1	0
Gfi1$^{36S/36S}$	80 ± 5	16 ± 5	3 ± 1	3 ± 1	1 ± 1

Quantification of the different cell types according to their morphology enumerated from bone marrow cytospins of the indicated mouse strains (n = 3 for all genotypes).
*Significant difference to *wt* mouse strain.

cells.[25,26] Similarly, a higher percentage of *Gfi1*$^{36N/36N}$ GMPs were undergoing cell cycling than in *Gfi1*$^{36S/36S}$ or *wt* mice, indicating that the GFI136N variant also causes a proliferative expansion of the GMP progenitor fraction (Figure 2C). Interestingly, this proliferative expansion of GMPs is also observable in Gfi1$^{36N/+}$ mice, which resembles the situation found in human AML patients that are heterozygous for this variant.[14] The fact that the presence of GFI136N affects specifically GMPs is of particular interest because it has been shown that, in humans as well as in mice, leukemic stem cells arise in the CMP and GMP fractions and that human AML stem cells can exhibit expression patterns similar to normal LMPPs and GMPs.[9-12]

GFI136N affects gene expression and function of GMPs

To understand why GFI136N but not GFI136S causes an expansion of GMPs, we compared genome-wide mRNA expression patterns of GMPs from *Gfi1*$^{36N/36N}$ and *Gfi1*$^{36S/36S}$ animals with those from *wt* and *Gfi1*$^{-/-}$ mice. Unsupervised hierarchical clustering of the expression levels of individual genes demonstrated a high similarity between GMPs from *Gfi1*$^{36S/36S}$ and *wt* mice (Figure 2D; see also "Gene expression array and real-time PCR") consistent with the notion that GFI136S is functionally equivalent to the endogenous murine Gfi1. In contrast, *Gfi1*$^{36N/36N}$ GMPs exhibited a genome-wide mRNA expression pattern that differed from that obtained with mRNA of *wt*, *Gfi1*$^{36S/36S}$ and even *Gfi1*$^{-/-}$ GMPs (Figure 2D). Using gene set enrichment analysis, we observed that the genes differentially expressed in GMPs from *Gfi1*$^{36S/36S}$ and *Gfi1*$^{36N/36N}$ mice showed a pattern reminiscent of the features of adult HSCs and contained a HoxA specific gene signature (Figure 2E-F). In addition, these differentially expressed genes were found to be part of KEGG pathways describing hematopoietic cell lineage determination, cytokine receptor interactions, Jak-STAT signaling, and cancer signaling (Figure 2G).

When we compared the lists of genes that were differentially expressed between GMPs from different mouse mutants (Figure 2H), the largest overlap was found when genes differentially expressed in GMPs from *Gfi1*$^{36N/36N}$ and *Gfi1*$^{36S/36S}$ mice were compared with those differentially expressed in GMPs from *Gfi1*$^{36N/36N}$ and *wt* mice (631 genes, Figure 2H). This indicated that *Gfi1*$^{36S/36S}$ and *wt* GMPs were similar in their expression pattern and that GMPs from *Gfi1*$^{36N/36N}$ mice clearly differed from *wt,* *Gfi1*$^{36S/36S}$, and even *Gfi1*$^{-/-}$ GMPs. This also suggested that the presence of GFI136N is not simply recapitulating Gfi1 deficiency but exerts a distinctly aberrant function

A gene set enrichment analysis indicated that Gfi136N cells have characteristics also found in HSCs. Hence, we tested the self-renewal capacity of GFI136N GMPs in colony replating assays and found that GFI136N-expressing GMPs generated more colonies than GFI136S expressing GMPs during the initial plating and the first replating (Figure 2I). However, the replating efficiency of GFI136N-expressing GMPs was exhausted after 3 platings similar to GFI136S GMPs (Figure 2I). Next, we transplanted GMPs sorted from Gfi1$^{36S/36S}$ or Gfi1$^{36N/36N}$ mice (both CD45.2$^+$) along with CD45.1$^+$ bone marrow carriers into sublethally irradiated CD45.1$^+$ animals and determined the frequency of CD45.2$^+$ GMPs in the recipients 24 days later. Consistent with published findings, no CD45.2$^+$ GFI136S expressing GMPs were detectable, but we found that ~ 1% of all GMPs of mice transplanted with GMPs from Gfi1$^{36N/36N}$ mice were CD45.2$^+$ (Figure 2K-L). This suggested that GMPs with GFI136N variant alleles not only expand because of higher proliferation but have gained a certain capacity of self-renewal that is not found in GMPs expressing the more common GFI136S form.

GFI136N derepresses Hoxa9 expression in GMPs by altering histone modifications

Expression of the Gfi1 target and known oncogene HoxA9 was significantly up-regulated in *Gfi1*$^{36N/36N}$ versus *wt* or *Gfi1*$^{36S/36S}$ GMPs (Figure 3A). *Hoxa9* is important for AML pathogenesis, and high levels of Hoxa9 or Hoxa9 fusion proteins are sufficient to induce AML in mice.[27,28] High Hoxa9 expression levels are characteristic for human AML stem cells[9] and correlate in AML patients with a poor prognosis.[29] Loss of Gfi1 leads to up-regulation of *Hoxa9* expression in GMPs (Figure 3A), probably contributing to the numeric expansion of these cells in Gfi1-deficient mice.[4] Although high Hoxa9 expression and GMP expansion are detectable in *Gfi1*$^{-/-}$ mice, these animals do not develop an AML. This is probably because Gfi1 also protects against apoptosis because the introduction of a Bcl-2 transgene leads to the development of a myeloproliferative disease in *Gfi1*$^{-/-}$ mice that resembles AML.[22]

It is known that Gfi1 represses transcription by recruiting histone-modifying enzymes, such as LSD1, G9a, and HDACs, to target gene promoters.[30,31] LSD1 and HDAC enable the demethylation of H3K4 and deacetylation of H3K9 residues, respectively, both markers associated with gene activation. In contrast, G9a catalyzes the methylation of H3K9 residues, which is associated with gene repression.[31] To test whether the GFI136N variant can affect histone modifications at the Hoxa9 locus, we sorted Lin$^-$, Sca1$^-$, ckit$^+$ cells (which contain GMPs) from bone marrow of *Gfi1*$^{36S/36S}$ and *Gfi1*$^{36N/36N}$ mice and performed ChIP with antibodies either recognizing the human GFI1 or methylated or acetylated H3K4 or H3K9 residues. We found that GFI136N bound to a lesser degree to the *Hoxa9* locus than GFI136S and that this correlated with a higher degree of H3K4 dimethylation, H3K9 acetylation, and lower H3K9 dimethylation at GFI1 binding sites at the Hoxa9 locus in GFI136N-expressing cells (Figure 3B-F). A similar finding could be found for GFI136N heterozygous mice (supplemental Figure 3). These data strongly suggest that the GFI136N variant is unable to regulate the expression of Hoxa9, which is a validated GFI1 target gene with high relevance for AML. As a result, the transcription of *Hoxa9* is not properly silenced in GMPs that carry a Gfi136N variant allele.

Albeit this inability of GFI136N to bind to the HoxA9 promoter, both GFI1 variants were still able to interact with LSD1 (Figure 3G) and other known cofactors, such as PU.1 (supplemental Figure 4). In addition, both GFI1 variants could bind to other direct Gfi1 target genes, such as *Id2* or *Gfi1*, itself at similar rates in thymocytes (Figure 3H).[16,17] In addition, GFI136S and GFI136N were both able to repress transcription of the human *Hoxa9* gene in a reporter gene assay (supplemental Figure 5). This suggested that the observed differences of GFI136S and GFI136N in their ability to regulate the *Hoxa9* locus are specific for GMPs and do not occur in other cell types. Hence, a cell type specific factor or pathway must exist that affects the 2 GFI1 variants differentially in GMPs.

Consistent with our observation with GMPs from *Gfi1*$^{36N/36N}$ mice, blast cells from *GFI1*$^{36N/36S}$ AML patients featured higher Hoxa9 expression levels than blast cells originating from *GFI1*$^{36S/36S}$ patients (Figure 3G), although the level of up-regulation was less pronounced in humans than in mice. In addition, in an independent cohort of 350 patients, Hoxa9 was among the 10 most up-regulated genes between *GFI1*$^{36N/36S}$ and *GFI1*$^{36S/36S}$ AML patients as determined by large-scale gene expression analyses (Table 3).[21] These

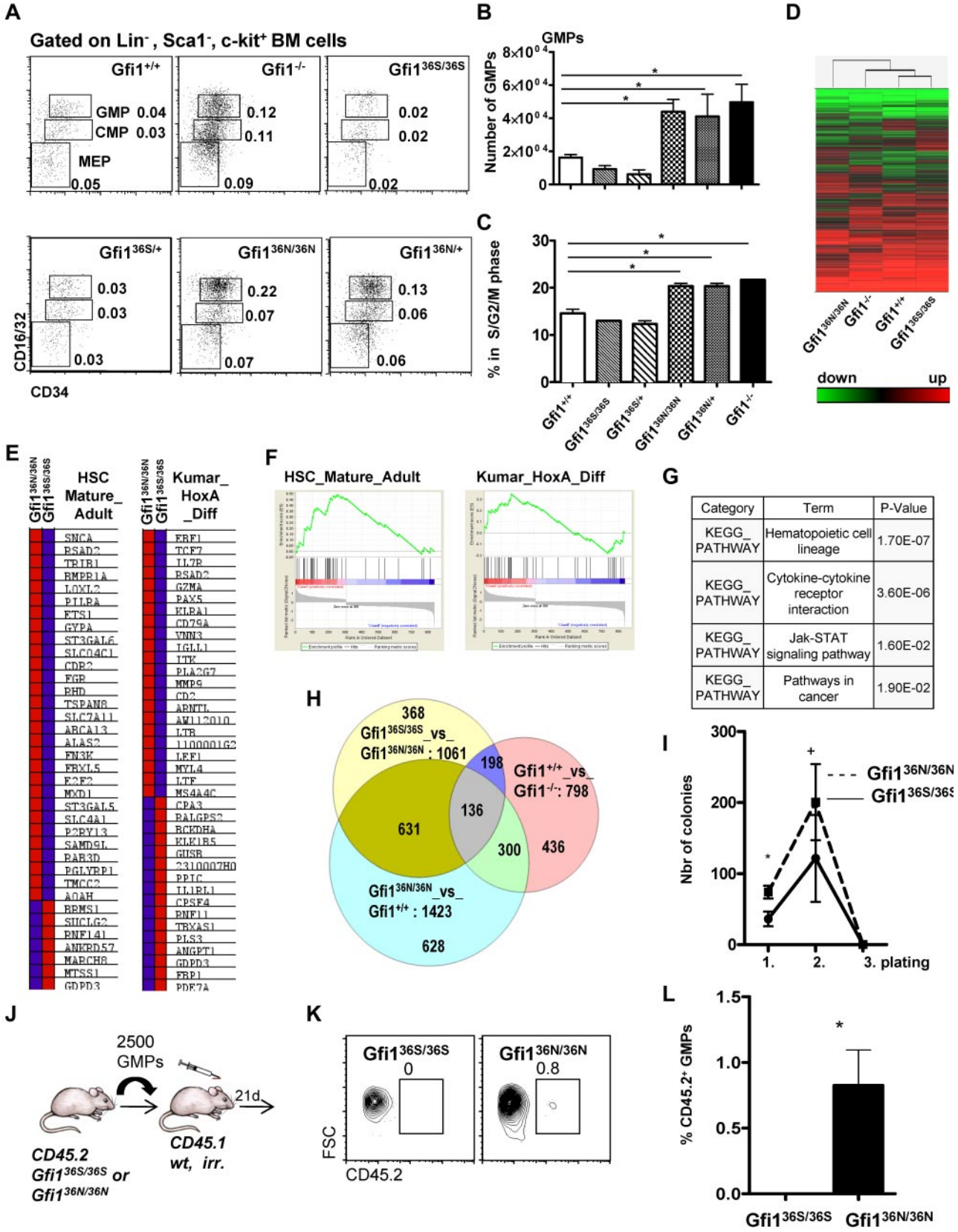

Figure 2. The presence of GFI136N affects the GMP bone marrow fraction in *Gfi1*$^{36N/36N}$ knock-in mice. (A) Representative flow cytometric analysis of CMPs, GMPs, and MEPs of the indicated mouse strains. Numbers indicate percentage of the different populations with regard to the total bone marrow cells. (B) Total number of GMPs in the different mouse strains (both hind limbs; n = 24 for *Gfi1*$^{+/+}$, n = 15 for *Gfi1*$^{-/-}$, n = 15 for *Gfi1*$^{36N/36N}$, n = 7 for *Gfi1*$^{36S/36S}$, n = 4 for *Gfi1*$^{36N/+}$, n = 3 for *Gfi1*$^{36N/+}$). *$P \leq .05$. (C) Cell cycle progression of the GMPs from the indicated strains (n = 5 for *Gfi1*$^{+/+}$, n = 3 for *Gfi1*$^{-/-}$, n = 5 for *Gfi1*$^{36N/36N}$, n = 5 for *Gfi1*$^{36S/36S}$, n = 5 for *Gfi1*$^{36N/+}$, n = 3 for *Gfi1*$^{36N/+}$). *$P \leq .05$. (D) Heat map representing the different mRNA expression profiles in GMPs from the indicated mouse strains. Genes expressed in GMPs at more than a 2-fold difference in the comparisons, *Gfi1*$^{-/-}$ vs *Gfi1*$^{+/+}$, *Gfi1*$^{36N/36N}$ vs *Gfi1*$^{36S/36S}$, or *Gfi1*$^{36N/36N}$ vs *Gfi1*$^{+/+}$, were analyzed by hierarchical clustering using Wards method

results and previous reports, which demonstrated that Hoxa9 up-regulation is indeed responsible for the expansion of the GMPs in Gfi1-deficient mice,[4] indicates that elevated Hoxa9 expression could play a major role in the pathogenesis of AML in GFI136N heterozygous patients. Based on these data and our findings with *Gfi1*$^{36N/36N}$ knock-in mice and in particular because Hoxa9 expression is directly linked to the development of AML,[4,27,32,33] we reasoned that the inability of GFI136N to repress Hoxa9 in GMPs may explain the association of the variant GFI136N allele with AML in human patients.

Presence of GFI136N induces epigenetic changes at a genome-wide level

We next tested whether the epigenetic changes associated with GFI136N were restricted to the Hoxa9 locus or whether they could be found at GFI1 binding sites throughout the genome. To determine genome-wide occupancy by Gfi1, we performed a ChIP-Seq experiment using Gfi1 antibodies and cells from murine AML induced by the MLL-Enl onco-fusion gene because large numbers of cells are required to efficiently immune-precipitate murine Gfi1 with currently available antibodies. We also performed ChIP-Seq experiments on sorted Lin$^-$, Sca1$^-$, ckit$^+$ cells from both *Gfi1*$^{36N/36N}$ and *Gfi1*$^{36S/36S}$ mice using antibodies recognizing H3K4 dimethylation.

These experiments demonstrated that Gfi1 indeed occupies the genomic regions of Hoxa9 and a number of other validated target genes, such as *Id2*, *Meis1*, *IL-6Ra*, *PU.1*, and *Pbx1* (Figure 4A-G). In addition, GFI136N-expressing cells showed a much higher degree of H3K4 dimethylation at the *Hoxa9* promoter, but also in the 5′region and within the Hoxa9 gene than cells that express the GFI136S form (Figure 4A), which is consistent with the ChIP-PCR results obtained with sorted GMPs (Figure 3B,D). Interestingly, similar epigenetic changes were also evident, albeit to a lesser degree, at other Gfi1 target genes, such as the *ID2* and *IL-6RA* locus, whereas other Gfi1 target genes, such as *Meis1*, *PU.1*, and *Pbx1*, showed no noticeable differences in H3K4 dimethylation when GFI136N was present (Figure 4B-F). A quantification of expression levels (fold up-regulation calculated using values from the GMP expression arrays) and H3K4 dimethylation (fold change calculated using peak areas) confirmed that the effect of the GFI136N variant was most pronounced at the *Hoxa9* locus.

GFI136N accelerates the onset of a myeloproliferative disorder

We reasoned that the up-regulation of Hoxa9 and the epigenetic changes in other genes, which play a role in AML, might render GFI136N-expressing GMPs more susceptible for a progression to a myeloid malignancy. To verify this hypothesis, we tested whether the presence of GFI136N could affect the malignancy of a myeloproliferative-like disease or its transformation into an AML in vivo. It is known that constitutive activation of K-RAS is a recurring oncogenic event in AML,[34] and transgenic mice carrying a conditional mutant *K-RAS*^{fsfK12D} allele (*K12D floxstopflox K-RAS*) allow develop a malignant myeloproliferative disease.[35-37] In this model, the K-RAS oncogene is activated after removal of a stop codon, which can be achieved by injecting MxCre, K-RAS^{fsfK12D} mice with poly(I:C; Figure 5A). We used this model and crossed wt, *Gfi1*$^{36N/+}$, *Gfi1*$^{36N/36N}$, and *Gfi1*$^{36S/+}$ mouse strains with MxCre, *K-RAS*^{fsfK12D} mice and injected offspring with poly(I:C) to induce expression of the mutated form of K-RAS (Figure 5A). All combinatorial mouse mutants died as expected from a fatal myeloproliferative disorder that was accompanied by an expansion of myeloid cells in the bone marrow, an infiltration of myeloid cells in the spleen, and the appearance of blast cells in the blood (Figure 5B-C). As control mice, we treated *Mx Cre tg Gfi1*$^{flox/flox}$ mice or wt mice with polyriboinosinic acid/polyribocytidylic acid and monitored their survival to exclude that a higher mortality might be related to Cre activation or to a toxic effect of poly(I:C). However, none of the control mice died of a myeloproliferative disease or any other disease and survived well beyond the observation period (Figure 5D). This excludes that polyriboinosinic acid/polyribocytidylic acid treatment or Cre activation interferes with the *K-RAS* induced disease. Whereas *Gfi1*$^{+/+}$ and G*fi1*$^{36S/+}$ mice developed a myeloproliferative disease within a similar median latency of 27 and 33 days, respectively, *Gfi1*$^{36N/+}$ and *Gfi1*$^{36N/36N}$ mice died significantly faster from this disease (18 for *Gfi1*$^{36N/+}$ and 16 days for *Gfi1*$^{36N/36N}$ mice, respectively, $P \leq .01$; Figure 5D; only data for *Gfi1*$^{36N/+}$ mice are shown). This indicates that heterozygosity of GFI136N suffices to accelerate a fatal myeloproliferative disorder in mice and further suggests that a causal relationship might exist between the variant GFI136N allele and fatal myeloproliferative diseases in humans.

Discussion

Our experiments provide evidence that the GFI136N variant affects the GMP bone marrow fraction, which has been recognized to be one of the original progenitors (besides CMPs and LMPPs) from which AML leukemic stem cells originate in humans and mice.[9-12] Our findings suggest that the presence of GFI136N changes the histone code in GMPs by retaining epigenetic activation marks at the *Hoxa9* locus, causing a continued, high level of Hoxa9 expression. In contrast, in wild type GMPs and in those expressing the more common GFI1 form (GFI136S), Hoxa9 is down-regulated in comparison. It has been shown that high levels of Hoxa9 increase the number of GMPs and confer an enhanced capacity for self-renewal to these cells.[4,9,27,32,33,38] GMPs expressing the GFI136N variant show, as predicted from their high Hoxa9 expression, a proliferative expansion, higher ability to form colonies in semisolid medium and a higher self-renewal capacity as their wt or GFI136S counterparts. It is thus conceivable that the presence of GFI136N enhances the risk that GMPs develop into a leukemic stem cell and eventually give rise to myeloid malignancies. Our experiments with the *K-RAS* model of a myeloproliferative disorder support this

Figure 2. (continued) (similarity measure: half square eucledian distance). (E-F) Gene set enrichment analysis showed that sets of genes differentially expressed in mature adult hematopoietic cells compared with stem cells (HSC_Mature_Adult) and in MLL-AF9 leukemia (Kumar_HoxA_Diff) are enriched in the list of genes that are differentially expressed between *Gfi1*$^{36S/36S}$ and *Gfi1*$^{36N/36N}$ GMPs. (G) Table of results of KEGG pathway analysis showing that genes differentially expressed between *Gfi1*$^{36S/36S}$ and *Gfi1*$^{36N/36N}$ GMPs fall into the indicated pathways, the one composing hematopoietic cell lineage genes being the most significant. (H) Venn diagram comparing the number of overlapping genes differentially expressed in GMPs from the indicated mouse strains. (I) A total of 450 GMPs from *Gfi1*$^{36S/36S}$ and *Gfi1*$^{36N/36N}$ mice were sorted directly on methylcellulose, and 20 000 cells were replated from the emerging colonies every 10 days (see also "In vitro colony assay"). *$P = .05$. n = 3 for all genotypes. (J) Schematic outline of transplantation experiment. A total of 2500 GMPs were sorted from Gfi1$^{36S/36S}$ or Gfi1$^{36N/36N}$ mice and transplanted together with 10^5 bone marrow cells from CD45.1$^+$ mice into lethally irradiated CD45.1$^+$ mice. (K) At 24 days after transplantation, the number of CD45.1$^+$ (all wt) and CD45.2$^+$ (either *Gfi1*$^{36S/36S}$ or *Gfi1*$^{36N/36N}$) GMPs was determined. (L-M) At 24 days after transplantation of either *Gfi1*$^{36S/36S}$ or *Gfi1*$^{36N/36N}$ CD45.2$^+$ GMPs, the percentage of CD45.2$^+$ GMPs was determined in the recipient mice. Whereas no CD45.2$^+$, *Gfi1*$^{36S/36S}$ GMPs were detectable, ~ 1% of the GMPs were CD45.2$^+$ *Gfi1*$^{36N/36N}$ GMPs.

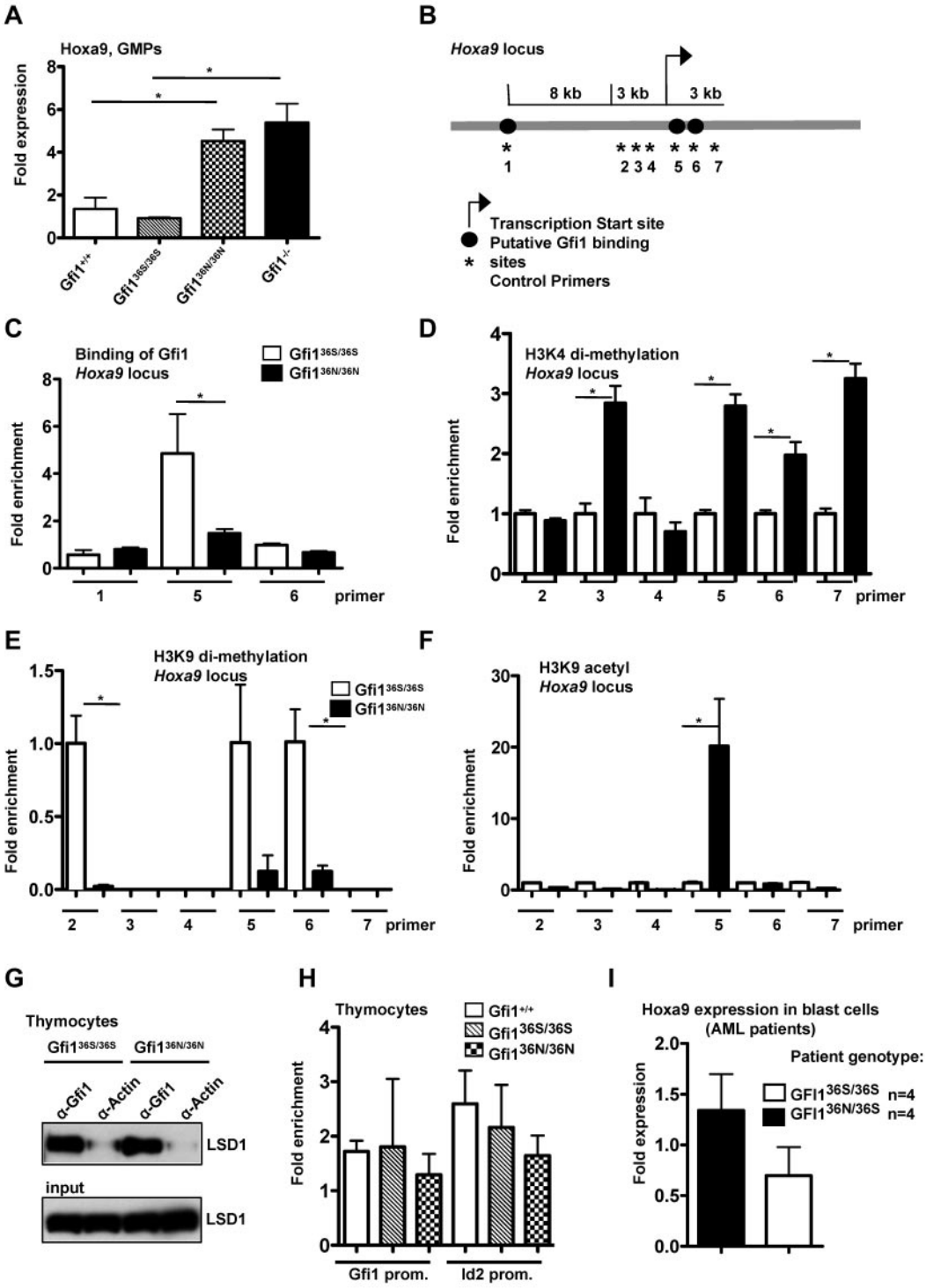

Figure 3. Deregulation of Hoxa9 expression and epigenetic modification in myeloid cells from *Gfi1*$^{36N/36N}$ knock-in mice. (A) *Hoxa9* mRNA expression was determined in GMPs by RT-PCR. One representative experiment (with triplicates for each experiment) from 2 independent experiments is shown. (B) Schematic representation of the *Hoxa9* locus. Numbers indicate the position of the primer pairs used for ChIP-PCR. (C) ChIP-PCR with sorted Lin$^-$, c-kit$^+$, Sca1$^-$ cells from the indicated mouse strains using an α-Gfi1 antibody. Shown is the representative result of 2 independent experiments, each done in triplicate (for location of primers see panel B). (D) ChIP-PCR with sorted Lin$^-$, c-kit$^+$, Sca1$^-$ cells from the indicated mouse strains using an α-H3K4 dimethyl-antibody (for locations of primers see panel B). Enrichment for Gfi136S is set at 1. (E) ChIP-PCR with sorted Lin$^-$, c-kit$^+$, Sca1$^-$ cells from the indicated mouse strains using an α-H3K9dimethyl-antibody (for locations of primers see panel B; for enrichment see panel D). (F) ChIP-PCR with sorted Lin$^-$, c-kit$^+$, Sca1$^-$ cells from the indicated mouse strains using an α-H3K9acetyl antibody (for locations of primers see panels B and D). (G) Immunoprecipitations (IP) using thymocyte extracts from the indicated mouse strains with an α-Gfi1 antibody. As control, an α-actin antibody was used. (H) ChIP-PCR with thymocytes using an anti-Gfi1 antibody (from left to right: *Gfi1*$^{+/+}$, *Gfi1*$^{36S/36S}$, *Gfi1*$^{36N/36N}$). Relative enrichment was determined by amplification with previously described primers (see "ChIP"). (I) Hoxa9 mRNA expression level was determined in blast cells of 4 *GFI1*$^{36S/36S}$ and 4 *GFI1*$^{36N/36S}$ AML patients ($P \leq .10$).

view, but additional future work with other models in particular those that elicit AML is required to confirm such a role of GFI136N. However, our results confirm the findings of Horman et al[4] that Gfi1 regulates the expression of Hoxa9 and that altered function of Gfi1, such as in case of Gfi136N or loss of Gfi1, leads to an accelerated onset of a myeloproliferative disease. We can also

Table 3. Up-regulated genes in human Gfi136N/36S AML blast cells

Gene	Fold change in Gfi1$^{36S/36N}$ versus GFI1$^{36S/36S}$ patients
SOCS2	2.05
MARCKS	2.02
*HOXA9**	1.87
CYBB	1.84
BASP1	1.84
SOCS2	1.82
RNASE6	1.8
DACH1	1.8
SERPINB2	1.79
MPEG1	1.79

List of the 10 most up-regulated genes comparing gene expression arrays of AML blast from patients heterozygous for *GFI136N* (n = 25) to AML blast from patients homozygous for *GFI136S* (n = 325).

observe the emergence of T-cell leukemia after transplanting bone marrow cells from mice expressing a mutant *K-RAS* oncogene, but not when Gfi1 is absent. In addition, Horman et al show experiments suggesting that Gfi1 deficiency converts a K-RAS–induced myeloproliferative disease into a transplantable AML.[4] The differences with regard to transplantation of Gfi1-deficient cells could be because of the fact, that in the experimental setting used here, constitutively and not conditionally Gfi1 deficient mice were used. It is thus possible that conditional ablation is less efficient and that a different Gfi1 dosage might have a different effect on KRA-transformed cells than a full, constitutive deletion of Gfi1.

The epigenetic changes observed at the *Hoxa9* locus also occur at other Gfi1 target genes in GMPs carrying variant GFI136N alleles, albeit at a lower level. It is possible that these changes are

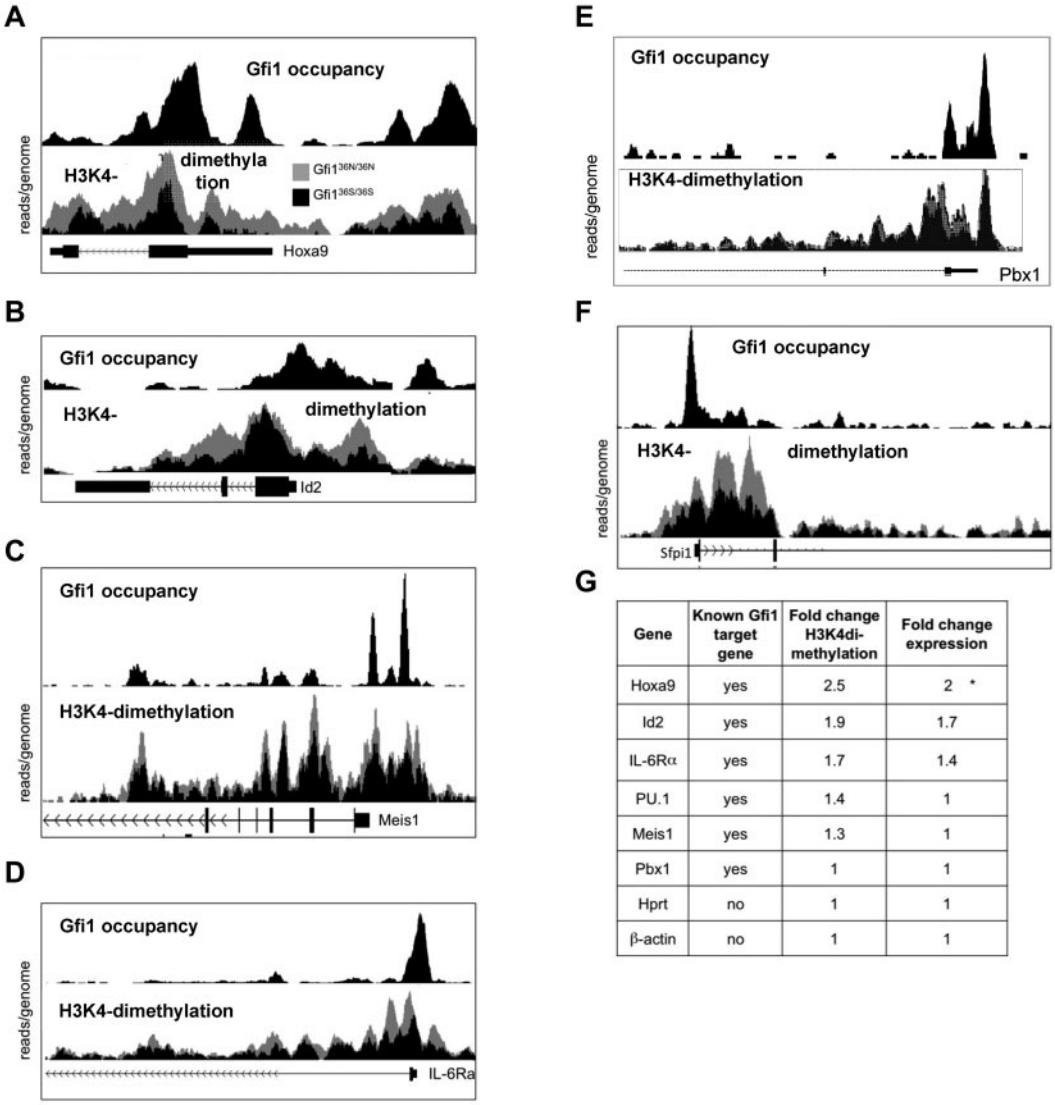

G

Gene	Known Gfi1 target gene	Fold change H3K4di-methylation	Fold change expression
Hoxa9	yes	2.5	2 *
Id2	yes	1.9	1.7
IL-6Rα	yes	1.7	1.4
PU.1	yes	1.4	1
Meis1	yes	1.3	1
Pbx1	yes	1	1
Hprt	no	1	1
β-actin	no	1	1

Figure 4. Presence of Gfi136N induces epigenetic changes at several loci. Result of the ChIP-Seq experiments indicating Gfi1 occupancy and histone H3 lysine 4 9H3K4) at selected gene loci. For the detection of H3K4 dimethylation, ChIP was performed with sorted Lin$^-$, c-kit$^+$, Sca1$^-$ cells from the indicated mouse strains using a α-H3K4 dimethyl antibody. For the detection of Gfi1, ChIP was performed with an α-Gfi1 antibody using MLL-ENL-transduced AML cells. After immunoprecipitation, DNA-protein complexes were subjected to high throughput sequencing to determine the genome-wide distribution of H3K4 dimethyl as well as of Gfi1 binding. In each figure, the top half represents the enrichment for Gfi1 binding and the lower half the distribution of H3K4dimethylation in cells from either *Gfi1$^{36N/36N}$* or *Gfi1$^{36S/36S}$* mice. The results of the H3K4dimethyl ChIP-Seq were normalized (see "ChIP seq"), and the curves of obtained with cells from the 2 different mouse strains were superimposed. The curves representing *Gfi1$^{36N/336N}$* cells appear in gray, the curves of Gfi1$^{36S/36S}$ in black. The following gene loci have been analyzed: Hoxa9 (A), *Id2* (B), *Meis1* (C), *IL-6Ra* (D), *PU.1* (E), and *Pbx1* (F). (G) Summary of changes in H3K4 dimethylation and expression of the indicated Gfi1 target and control genes. The fold change in H3K4dimethylation between cells from Gfi1$^{36N/36N}$ and Gfi1$^{36S/36S}$ mice was calculated by dividing the areas under the respective curves. The area under the curves was determined using the TL-100 Version 2008 software from Non-Linear Dynamics. Fold change expression of the indicated genes between cells from *Gfi1$^{36N/36N}$* and *Gfi1$^{36S/36S}$* mice was calculated by dividing the absolute expression levels obtained from the DNA microarray expression analysis (Figure 2D).

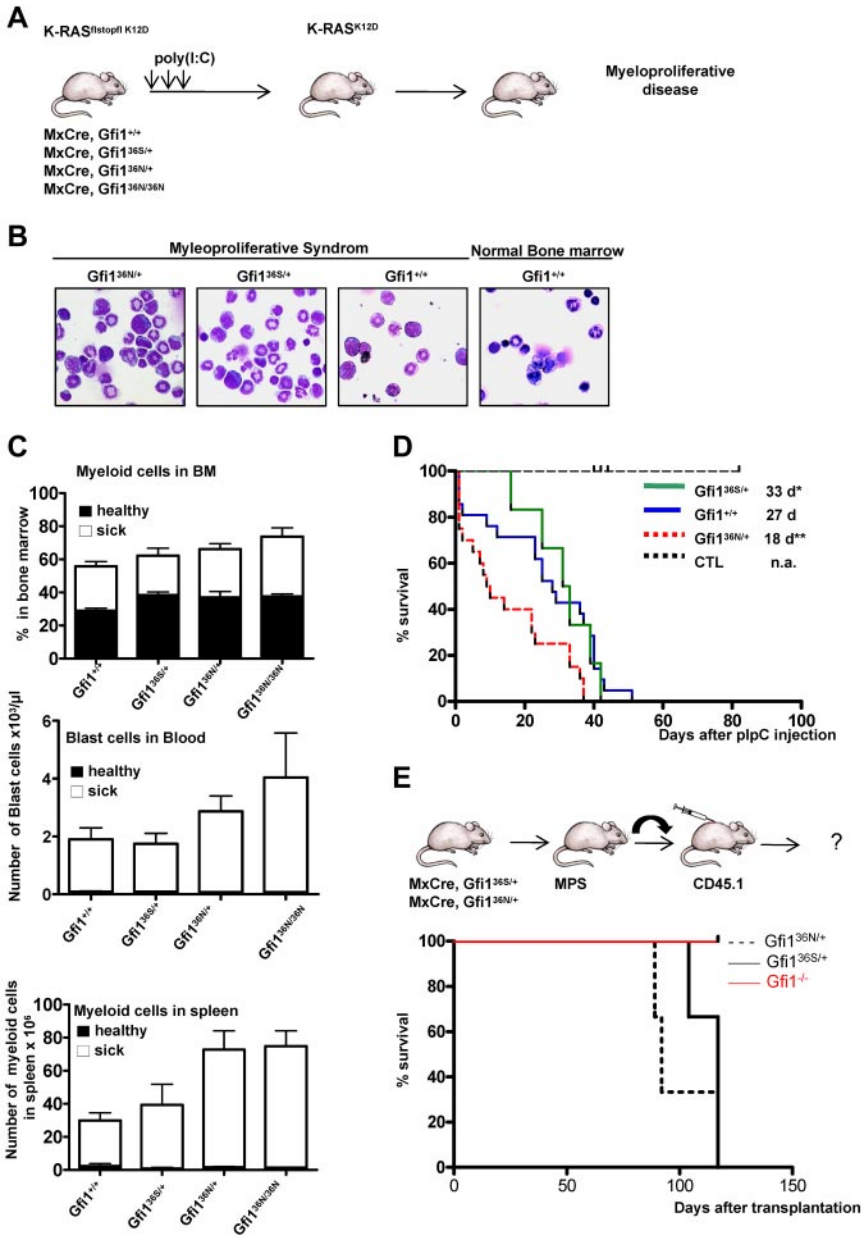

Figure 5. Accelerated onset of a myeloproliferative disorder in the presence of GFI136N. (A) Experimental setup to induce expression of a mutated K-RAS^{K12D} transgene. (B) Representative bone marrow cytospins of moribund mice with the indicated genotypes (original magnification ×100, Leitz DMRB from Leica, Micropublisher digital color camera, QImaging). (C) Frequency of myeloid and blast cells in healthy (dark bar) and sick mice (white bar). Top panel: Percentage of myeloid cells in the bone marrow (healthy mice: n = 18 *Gfi1*$^{+/+}$, n = 6 *Gfi1*$^{36N/36N}$, n = 3 *Gfi1*$^{36S/+}$, n = 3 *Gfi1*$^{36N/+}$; sick mice: n = 15 *Gfi1*$^{+/+}$, n = 8 *Gfi1*$^{36N/36N}$, n = 5 *Gfi1*$^{36S/+}$, n = 15 *Gfi1*$^{36N/+}$). Middle panel: Number of blast cells per microliter of blood, healthy mice: n = 21 *Gfi1*$^{+/+}$, n = 5 *Gfi1*$^{36N/36N}$, n = 3 *Gfi1*$^{36S/+}$, n = 4 *Gfi1*$^{36N/+}$; sick mice: n = 17 *Gfi1*$^{+/+}$, n = 5 *Gfi1*$^{36N/36N}$, n = 5 *Gfi1*$^{36S/+}$, n = 7 *Gfi1*$^{36N/+}$). Bottom panel: Total number of myeloid cells in the spleen (healthy mice: n = 21 for *Gfi1*$^{+/+}$, n = 3 for *Gfi1*$^{36N/36N}$, n = 3 for *Gfi1*$^{36S/+}$, n = 3 for *Gfi1*$^{36N/+}$; sick mice: n = 16 *Gfi1*$^{+/+}$, n = 8 *Gfi1*$^{36N/36N}$, n = 5 *Gfi1*$^{36S/+}$, n = 14 *Gfi1*$^{36N/+}$). All sick mice carried both the MxCre transgene and the K-RAS$^{flstopfl\ K12D}$ allele. (D) Kaplan-Meier survival curve of different strains (n = 12 for control mice, n = 22 for *Gfi1*$^{+/+}$, n = 7 for *Gfi1*$^{36S/+}$, n = 22 for *Gfi1*$^{36N/+}$). $P \leq .01$ between Gfi1$^{36N/+}$ and Gfi1$^{+/+}$. $P \leq .04$ between Gfi1$^{36N/+}$ and Gfi1$^{36S/+}$. The cohort of control mice (CTL) was composed of 2 different subgroups. One group (n = 8) consisted of *Mx Cre tg Gfi1*$^{flox/flox}$ mice, which were injected with poly(I:C) to exclude that a higher mortality of mice might be related to Cre activation or toxicity of poly(I:C). The second subgroup (n = 6) consisted of wt mice, which were injected with poly(I:C) also to monitor toxic effects of poly(I:C). With the exception of the control mice, all other mice carried an MxCre transgene and a *K-RAS*$^{flstopfl\ K12D}$ allele. (E) Approximately 2×10^6 bone marrow cells of moribund mice (see panel D) with the indicated genotypes were transplanted alongside 10^5 CD45.1$^+$ carrier bone marrow cells into sublethally irradiated CD45.1$^+$ mice. Mice were then subsequently observed for emergence of disease; n = 3 for all genotypes. *$P \leq .05$.

also critical for the accelerated development of a myeloproliferative disease in *Gfi1*$^{36N/36N}$ or *Gfi1*$^{36N/+}$ mice. The extent by which H3K4 dimethylation is retained in GFI136N cells is however striking and suggests that the aberrant function of the GFI136N variant is either specifically targeted to the Hoxa9 locus or is most visible at this locus for yet unknown reasons. The potential relevance of elevated Hoxa9 levels in our mouse model with regard to the development of human AML is also underscored by our finding that we observed in 2 independent cohorts of AML patients a tendency for higher Hoxa9 expression levels in blast cells carrying one *GFI136N* allele compared with blasts homozygous for *GFI136S*. Finally, the causative role of Hoxa9 overexpression in the pathogenesis of human and murine myeloid leukemia has been demonstrated in many different experiments and animal models and high Hoxa9 expression levels have been documented at many occasions in human AML blasts.[4,9,22,27,29,32,33,38] Based on these data and our own findings, it is conceivable that the presence of the GFI136N variant causes elevated levels of Hoxa9, which is responsible for the proliferative expansion and higher self-renewal capacity of GMPs, setting the stage for a myeloproliferative disease and eventually for AML, if other cooperating events occur.

The analysis of 6 different Gfi1 target genes (*Hoxa9*, *Id2*, *IL-6Ra*, *PU.1*, *Meis1*, and *Pbx1*) with regard to expression changes and altered H3K4 dimethylation pattern in GFI136N cells showed that the best correlation was found for the *Hoxa9* locus. Hoxa9 expression was up-regulated and had higher H3K4 dimethylation in GFI136N cells. Only *Id2* and *IL-6Ra* showed a similar correlation, but not the other target genes. Although the exact reasons for this remain to be elucidated, it is possible that these genes are subject to control by other histone modifiers and transcription factors. This may also explain why the GFI136N variant does not cause AML but rather accelerates the development of an oncogene-driven nonmalignant myeloproliferative disease and that additional events leading to the deregulation of other AML-related genes must take

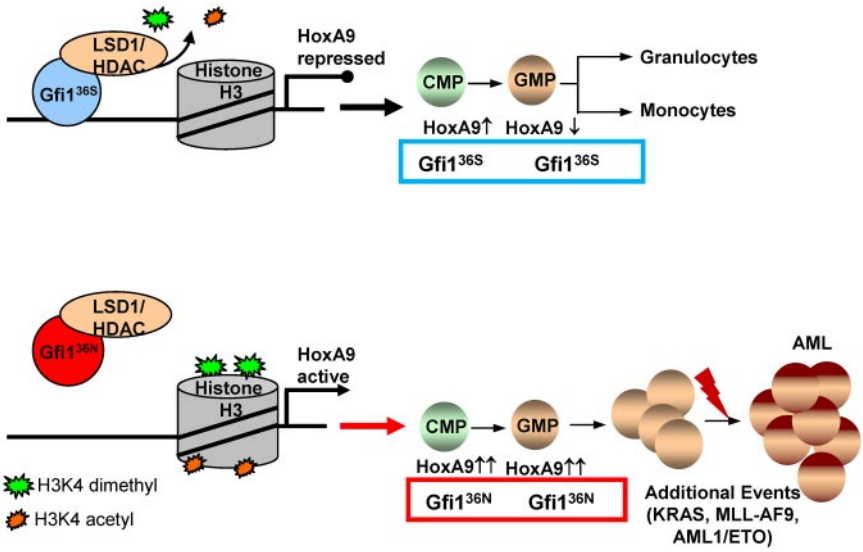

Figure 6. The role of the GFI136N variant in the development of a myeloproliferative disorder that may lead to AML. Proposed model for the function of the GFI136N variant: diminished binding of GFI136N to the *Hoxa9* locus as well as to other gene promoters results in epigenetic changes leading to deregulation of expression, in particular of the Hoxa9 gene and subsequently to a proliferative expansion of the GMPs. This effect of the GFI136N variant can increase the likelihood that an AML develops, if other cooperating events occur.

place before an AML develops, even in GFI136N-expressing cells. In addition, no disease phenotype could be observed in cohorts of mice homozygous or heterozygous for the Gfi136N variant allele after 1 year. Hence, the presence of Gfi136N alone without any additional mutations is not sufficient to cause AML in mice. This is also consistent with the fact that 3%-5% of all healthy persons carry this variant, but the overall incidence rate for AML with 3.6 per 100 000 men and women per year is much lower.

It is important to note that the association between the GFI136N variant and AML was found with patients heterozygous for the variant allele (ie, *GFI136N/GFI136S*) because only 1 homozygous patient was found in a large cohort of >1000 individuals.[14] Similarly, in our present study, we find that the proliferative expansion of GMPs and the faster onset of a myeloproliferative disease already occurs in mice heterozygous for the GFI136N allele (ie, in $Gfi1^{36N/wt}$ knock-in mice) and that the epigenetic changes at the *HoxA9* locus can also be found in *GFI136N* heterozygous mice. One possible explanation would be that the GFI136N variant form may cause a loss of function as a dominant negative mutant. Two findings would argue against such a role: first, our gene expression profiling suggests that the Gfi136N variant does not cause a loss of function, but Gfi136N homozygous GMP mice have a distinct expression pattern different from Gfi1 deficient GMPs. Second, although $Gfi1^{-/-}$ mice feature increased expression of Hoxa9 in GMPs,[4,22] as a result of this proliferative expansion of GMPs, they never develop an AML or an AML-like disease. This can be explained by the fact that Gfi1 also inhibits apoptosis and, as a result of this, loss of Gfi1 is associated with increased cell death, preventing emergence of a full-blown AML from the GMP fraction.[22] In line with this, constitutive overexpression of the antiapoptotic factor Bcl-2 in Gfi1-deficient mice causes a fatal myeloproliferative disorder resembling AML.[4,22]

Although Gfi136N is unable to repress Hoxa9 expression in GMPs, it can still protect against apoptosis (data not shown), and GMPs from $Gfi1^{36N/36N}$ mice are in this respect different from $Gfi1^{-/-}$ GMPs. Because the GFI136N variant has lost the function to repress *Hoxa9* in GMPs but retains its capacity to protect GMPs against apoptosis, it is possible that the deregulation of Hoxa9 and possibly other genes that remain to be identified confer an increased self-renewal capacity to GFI136N GMPs as is evident from colony replating and transplantation experiments. This and the increased number of GMPs may increase the likelihood of malignant transformation because the higher number of GMPs expands the pool of target cells. Similar findings have been reported for other mutations, which have been shown to induce AML by increasing the number of the cells, from which AML can arise.[39] The presence of GFI136N could increase the likelihood of for a premalignant disease, such as a myeloproliferative disease to occur, which then might develop into an AML, but only if additional mutations occur (Figure 6).

Our observations support an emerging concept that epigenetic changes and, as a result of this, reprogramming of gene expression patterns significantly contribute to the development of diseases and to malignant transformation.[40-50] As an example, we show here how an SNP that causes the expression of a variant form of a transcription factor (GFI136N) leads to specific epigenetic alterations and as a result of these changes might render myeloid precursors more susceptible to develop more quickly into preleukemic cells when an oncogenic event has occurred. To our knowledge, this is the first report of a mouse model, in which the introduction of a human coding SNP accelerates a myeloproliferative disease by inducing epigenetic changes. Our experiments support the notion that the epigenetic changes that occur in the presence of GFI136N lead to Hoxa9 up-regulation and potentially to the altered expression of other genes. This changes the overall gene expression pattern causing an altered function of GMPs, which is a cell population, from which in human and mice myeloproliferative disorders can arise. More research is needed to fully clarify the apparent locus specific function of the GFI136N variant. Our GFI136N or 36S knock-in mice already offer the possibility for further investigation and for the testing new therapeutic strategies targeting epigenetic changes in preleukemic cells.

Acknowledgments

The authors thank Mathieu Lapointe, Saskia Grunwald, and Rachel Bastien for technical assistance; Nancy Laverriere, Marlène Bernier, Marie-Claude Lavallée, and Mélanie St-Germain for excellent animal care; Eric Massicotte and Julie Lord for FACS and cell sorting; Odile Neyret for performing ChIPs; and Polly Chen for MLL-ENL transduced bone-marrow cells.

This work was supported by the Cancer Research Society, Canada (T.M.). J.S. and F.J.C.-N. were supported by Leukemia and Lymphoma Research United Kingdom. E.D. was supported by the Cambridge Stem Cell Center. R.H. was supported by the NIHR Cambridge Biomedical Research Center. C.K. was supported by the Cole Foundation (fellowship), the University Clinic of Essen (IFZ fellowship), and the German Cancer fund (Max-Eder-fellowship). M.-C.G. was supported by the CIHR (fellowship). T.M. was supported by a Tier 1 Canada Research Chair, the CIHR (MOP-84328), and the Cancer Research Society (Canada).

Authorship

Contribution: C.K. designed and performed research, analyzed data, and wrote the manuscript; J.K., L.V., M.-C.G., J.S., F.B., F.J.C.-N., E.D., R.H., and R.C. performed research, analyzed data, and edited the manuscript; B.A.v.d.R., J.H.J., B.L., J.K.P., H.L.G., S.E.M., and C.V.P. provided vital reagents; U.D. performed research, analyzed data, and provided funding; and B.G. and T.M. designed research, analyzed data, wrote the manuscript, and provided funding.

Conflict-of-interest disclosure: The authors declare no competing financial interests.

Correspondence: Bertie Göttgens, Cambridge University, Department of Haematology, Cambridge Institute for Medical Research, Hills Road, Cambridge CB2 0XY, United Kingdom; e-mail: bg200@cam.ac.uk; and Tarik Möröy, Institut de recherches cliniques de Montréal, 110, Avenue des Pins Ouest, Montréal, QC, Canada H2W 1R7; e-mail: tarik.moroy@ircm.qc.ca.

References

1. Phelan JD, Shroyer NF, Cook T, Gebelein B, Grimes HL. Gfi1-cells and circuits: unraveling transcriptional networks of development and disease. *Curr Opin Hematol.* 2010;17(4):300-307.
2. van der Meer LT, Jansen JH, van der Reijden BA. Gfi1 and Gfi1b: key regulators of hematopoiesis. *Leukemia.* 2010;24(11):1834-1843.
3. Karsunky H, Zeng H, Schmidt T, et al. Inflammatory reactions and severe neutropenia in mice lacking the transcriptional repressor Gfi1. *Nat Genet.* 2002;30(3):295-300.
4. Horman SR, Velu CS, Chaubey A, et al. Gfi1 integrates progenitor versus granulocytic transcriptional programming. *Blood.* 2009;123(22):5466-5475.
5. Velu CS, Baktula AM, Grimes HL. Gfi1 regulates miR-21 and miR-196b to control myelopoiesis. *Blood.* 2009;113(19):4720-4728.
6. Hock H, Hamblen MJ, Rooke HM, et al. Intrinsic requirement for zinc finger transcription factor Gfi-1 in neutrophil differentiation. *Immunity.* 2003; 18(1):109-120.
7. de la Luz Sierra M, Sakakibara S, Gasperini P, et al. The transcription factor Gfi1 regulates G-CSF signaling and neutrophil development through the Ras activator RasGRP1. *Blood.* 2010;115(19):3970-3979.
8. Person RE, Li FQ, Duan Z, et al. Mutations in proto-oncogene GFI1 cause human neutropenia and target ELA2. *Nat Genet.* 2003;34(3):308-312.
9. Goardon N, Marchi E, Atzberger A, et al. Coexistence of LMPP-like and GMP-like leukemia stem cells in acute myeloid leukemia. *Cancer Cell.* 2011;19(1):138-152.
10. Cozzio A, Passegue E, Ayton PM, Karsunky H, Cleary ML, Weissman IL. Similar MLL-associated leukemias arising from self-renewing stem cells and short-lived myeloid progenitors. *Genes Dev.* 2003;17(24):3029-3035.
11. Krivtsov AV, Twomey D, Feng Z, et al. Transformation from committed progenitor to leukaemia stem cell initiated by MLL-AF9. *Nature.* 2006; 442(7104):818-822.
12. Yeung J, Esposito MT, Gandillet A, et al. Beta-catenin mediates the establishment and drug resistance of MLL leukemic stem cells. *Cancer Cell.* 2010;18(6):606-618.
13. Heuser M, Yun H, Berg T, et al. Cell of origin in AML: susceptibility to MN1-induced transformation is regulated by the MEIS1/AbdB-like HOX protein complex. *Cancer Cell.* 2011;20(1):39-52.
14. Khandanpour C, Thiede C, Valk PJ, et al. A variant allele of Growth Factor Independence 1 (GFI1) is associated with acute myeloid leukemia. *Blood.* 2010;115(12):2462-2472.
15. Fiolka K, Hertzano R, Vassen L, et al. Gfi1 and Gfi1b act equivalently in haematopoiesis, but have distinct, non-overlapping functions in inner ear development. *EMBO Rep.* 2006;7(3):326-333.
16. Yucel R, Kosan C, Heyd F, Moroy T. Gfi1:green fluorescent protein knock-in mutant reveals differential expression and autoregulation of the growth factor independence 1 (Gfi1) gene during lymphocyte development. *J Biol Chem.* 2004; 279(39):40906-40917.
17. Li H, Ji M, Klarmann KD, Keller JR. Repression of Id2 expression by Gfi-1 is required for B cell and myeloid development. *Blood.* 2010;116(7):1060-1069.
18. Forsberg EC, Downs KM, Bresnick EH. Direct interaction of NF-E2 with hypersensitive site 2 of the beta-globin locus control region in living cells. *Blood.* 2000;96(1):334-339.
19. Langmead B. Aligning short sequencing reads with Bowtie. *Curr Protoc Bioinformatics.* 2010; Chapter 11:Unit 11 17.
20. Wilson NK, Miranda-Saavedra D, Kinston S, et al. The transcriptional program controlled by the stem cell leukemia gene Scl/Tal1 during early embryonic hematopoietic development. *Blood.* 2009; 113(22):5456-5465.
21. Valk PJ, Verhaak RG, Beijen MA, et al. Prognostically useful gene-expression profiles in acute myeloid leukemia. *N Engl J Med.* 2004;350(16): 1617-1628.
22. Khandanpour C, Kosan C, Gaudreau MC, et al. Growth factor independence 1 (Gfi1) protects hematopoietic stem cells against apoptosis but also prevents the development of a myeloproliferative-like disease. *Stem Cells.* 2011;29(2):376-385.
23. Akashi K, Traver D, Miyamoto T, Weissman IL. A clonogenic common myeloid progenitor that gives rise to all myeloid lineages. *Nature.* 2000; 404(6774):193-197.
24. Khandanpour C, Sharif-Askari E, Vassen L, et al. Evidence that growth factor independence 1b regulates dormancy and peripheral blood mobilization of hematopoietic stem cells. *Blood.* 2010; 116(24):5149-5161.
25. Zeng H, Yucel R, Kosan C, Klein-Hitpass L, Moroy T. Transcription factor Gfi1 regulates self-renewal and engraftment of hematopoietic stem cells. *EMBO J.* 2004;23(20):4116-4125.
26. Hock H, Hamblen MJ, Rooke HM, et al. Gfi-1 restricts proliferation and preserves functional integrity of haematopoietic stem cells. *Nature.* 2004;431(7011):1002-1007.
27. Kroon E, Thorsteinsdottir U, Mayotte N, Nakamura T, Sauvageau G. NUP98-HOXA9 expression in hemopoietic stem cells induces chronic and acute myeloid leukemias in mice. *EMBO J.* 2001;20(3):350-361.
28. Muntean AG, Tan J, Sitwala K, et al. The PAF complex synergizes with MLL fusion proteins at HOX loci to promote leukemogenesis. *Cancer Cell.* 2010;17(6):609-621.
29. Andreeff M, Ruvolo V, Gadgil S, et al. HOX expression patterns identify a common signature for favorable AML. *Leukemia.* 2008;22(11):2041-2047.
30. Duan Z, Zarebski A, Montoya-Durango D, Grimes HL, Horwitz M. Gfi1 coordinates epigenetic repression of p21Cip/WAF1 by recruitment of histone lysine methyltransferase G9a and histone deacetylase 1. *Mol Cell Biol.* 2005;25(23): 10338-10351.
31. Saleque S, Kim J, Rooke HM, Orkin SH. Epigenetic regulation of hematopoietic differentiation by Gfi-1 and Gfi-1b is mediated by the cofactors CoREST and LSD1. *Mol Cell.* 2007;27(4):562-572.
32. Faber J, Krivtsov AV, Stubbs MC, et al. HOXA9 is required for survival in human MLL-rearranged acute leukemias. *Blood.* 2009;113(11):2375-2385.
33. Wang Y, Krivtsov AV, Sinha AU, et al. The Wnt/beta-catenin pathway is required for the development of leukemia stem cells in AML. *Science.* 2010;327(5973):1650-1653.
34. Bowen DT, Frew ME, Hills R, et al. RAS mutation in acute myeloid leukemia is associated with distinct cytogenetic subgroups but does not influence outcome in patients younger than 60 years. *Blood.* 2005;106(6):2113-2119.
35. Braun BS, Tuveson DA, Kong N, et al. Somatic activation of oncogenic Kras in hematopoietic cells initiates a rapidly fatal myeloproliferative disorder. *Proc Natl Acad Sci U S A.* 2004;101(2): 597-602.
36. Chan IT, Kutok JL, Williams IR, et al. Conditional expression of oncogenic K-ras from its endogenous promoter induces a myeloproliferative disease. *J Clin Invest.* 2004;113(4):528-538.
37. Sabnis AJ, Cheung LS, Dail M, et al. Oncogenic Kras initiates leukemia in hematopoietic stem cells. *PLoS Biol.* 2009;7(3):e59.
38. Kroon E, Krosl J, Thorsteinsdottir U, Baban S, Buchberg AM, Sauvageau G. Hoxa9 transforms primary bone marrow cells through specific collaboration with Meis1a but not Pbx1b. *EMBO J.* 1998;17(13):3714-3725.
39. Klinakis A, Lobry C, Abdel-Wahab O, et al. A novel tumour-suppressor function for the Notch pathway in myeloid leukaemia. *Nature.* 2011; 473(7346):230-233.
40. Esteller M. Epigenetics in cancer. *N Engl J Med.* 2008;358(11):1148-1159.
41. Krivtsov AV, Feng Z, Lemieux ME, et al. H3K79 methylation profiles define murine and human MLL-AF4 leukemias. *Cancer Cell.* 2008;14(5): 355-368.
42. Bonadies N, Foster SD, Chan WI, et al. Genome-wide analysis of transcriptional reprogramming in mouse models of acute myeloid leukaemia. *PLoS One.* 2011;6(1):e16330.

43. Plass C, Oakes C, Blum W, Marcucci G. Epigenetics in acute myeloid leukemia. *Semin Oncol.* 2008;35(4):378-387.

44. Abdel-Wahab O, Levine RL. Metabolism and the leukemic stem cell. *J Exp Med.* 2010;207(4):677-680.

45. Scandura JM, Roboz GJ, Moh M, et al. Phase 1 study of epigenetic priming with decitabine prior to standard induction chemotherapy for patients with AML. *Blood.* 2011;118(6):1472-1480.

46. Theilgaard-Monch K, Boultwood J, Ferrari S, et al. Gene expression profiling in MDS and AML: potential and future avenues. *Leukemia.* 2011; 25(6):909-920.

47. Wong KY, So CC, Loong F, et al. Epigenetic inactivation of the miR-124-1 in haematological malignancies. *PLoS One.* 2011;6(4):e19027.

48. Yan XJ, Xu J, Gu ZH, et al. Exome sequencing identifies somatic mutations of DNA methyltransferase gene DNMT3A in acute monocytic leukemia. *Nat Genet.* 2011;43(4):309-315.

49. Agrawal-Singh S, Isken F, Agelopoulos K, et al. Genome-wide analysis of histone H3 acetylation patterns in AML identifies PRDX2 as an epigenetically silenced tumor suppressor gene. *Blood.* 2012;119(10):2346-2357.

50. Schenk T, Chen WC, Gollner S, et al. Inhibition of the LSD1 (KDM1A) demethylase reactivates the all-trans-retinoic acid differentiation pathway in acute myeloid leukemia. *Nat Med.* 2012;18(4): 605-611.